AJNR Am J Neuroradiol 26:496–501, March 2005

Case Report

Fibrocartilaginous Embolization to the Spinal Cord: Serial MR Imaging Monitoring and Pathologic Study

Thierry P. Duprez, Leslie Danvoye, Danielle Hernalsteen, Guy Cosnard, Christian J. Sindic, and Catherine Godfraind

Summary: We report the serial MR imaging and neuropathologic findings in a patient with fibrocartilaginous embolism to the spinal cord, presumptively originating from vertebral body endplates. Extensive increased T2 signal intensity, minimal contrast enhancing foci, concomitant vertebral body bone marrow infarction, and terminal cord hemorrhagic necrosis were the main MR imaging features. Pathologic examination of the cord demonstrated arteriolar occlusions by chondrocytic thrombi resulting in hemorrhagic necrosis.

Fibrocartilaginous embolization (FCE) to the spinal cord is a rare condition described in the early 1960s by Naiman et al (1) and by Laterre (2). So far, fewer than 30 such cases have been reported in the human medical literature, and all but one was identified at necropsy (3–5). This pathologic condition has also been described in the veterinary literature (6). A case studied by serial MR imaging was reported in 1991 by Mikulis et al (4, 7) in a histologically proven case of FCE to the spinal cord. Others have presumptively described FCE-related spinal cord infarction with the following clinical triad: 1) rapidly progressive paraplegia shortly after an episode of back pain (mostly after a minor trauma); 2) negative CSF examination; and 3) MR images showing cord swelling and increased T2 signal intensity together with intersomatic disk collapse or nucleus pulposus herniation into the adjacent vertebral body endplate (8–11).

Case Report

A 78-year-old woman, who had no significant medical history except for moderate and uncomplicated arterial hypertension, developed sudden paraplegia. The patient was admitted 6 hours after the onset of symptoms with normal consciousness but mild retro- and/or anterograde amnesia and spatial disorientation, which were interpreted as resulting from a fall a few days earlier. Neurologic examination revealed paraplegia prominently affecting the distal segments of the lower limbs with a strength ranging from 0 (distal muscles) to 3 (proximal ones). Knee reflexes were bilaterally weak, and the ankle reflexes were absent.

Plantar reflexes were unobtainable. A sensory level for pain and temperature was present from the L4 to the S5 level, mainly on the left side. The patient also suffered from urinary retention and fecal incontinence. MR imaging examination on admission demonstrated thin linear ependymal contrast enhancement on postcontrast T1-weighted images and slightly increased T2 signal intensity of the conus terminalis. An incidental hydrosyringomyelitic (HSM) cavity extending from Th7-Th8 to Th11 was present (Fig 1). Findings on CSF examination were normal except for a slightly elevated protein concentration at 58 mg/dL (normal range, 15–45 mg/dL). Because the patient's clinical status failed to improve, both examinations were repeated 5 days later.

Increased signal intensity within the conus had become obvious on the basis of T2-weighted imaging findings, strongly suggesting either an inflammatory or ischemic process (Fig 2). A concomitantly repeated CSF analysis remained unremarkable (i.e., no pleocytosis), thereby ruling out an inflammatory hypothesis. Further spinal follow-up MR imaging examinations demonstrated additional features, including anterior tilting of the tip of the edematous conus, upward extension of the T2 signal intensity abnormalities reflecting progression of edema and subsequent collapse of the pre-existing HSM cavity by the swollen surrounding parenchyma, enhancement of the cauda equina, foci of hematomyelic blood cord barrier disruption, small foci of bone marrow infarction within adjacent vertebral bodies, and a significant evolution from a homogeneous T2 hyperintensity of the diseased segments of the cord to a heterogeneous one, probably reflecting petechial transformation of the infarct (Figs 2A and 3B). MR imaging examination 3 days before death showed increased T1 signal intensity of the conal parenchyma and absence of significant contrast enhancement after gadolinium chelate perfusion, except for the pia (Fig 4). The patient died of a massive pulmonary embolism on the 28th day after admission; before there was no improvement of the paraplegia. Pathologic examination demonstrated both hemorrhagic necrosis and epithelialized embolic foci containing chondrocytes occluding microarterioles, leading to the definite diagnosis of FCE of the spinal cord and, probably, the vertebral bone marrow (Fig 5).

Discussion

Fewer than 30 cases of FCE resulting in spinal cord infarction have been reported in the human pathologic literature, and all but one of the cases was proven by postmortem pathologic examination of the cord (3–5). In our patient, definite etiologic diagnosis of "myelitis" remained speculative until necropsy was performed. For 2 decades, MR imaging has demonstrated high sensitivity in depicting spinal cord pathologic processes, but suffers lower specificity because

Received March 21, 2004; accepted May 13.

From the Departments of Radiology and Medical Imaging (T.P.D., D.H., G.C.), Neurology (L.D., C.J.S.), and Neuropathology (C.G.), Université catholique de Louvain, Cliniques universitaires Saint-Luc, Brussels, Belgium.

Address correspondence to Thierry P. Duprez, MD, Department of Radiology and Medical Imaging, Université catholique de Louvain, Avenue Hippocrate, 10, 1200-Brussels, Belgium.

© American Society of Neuroradiology

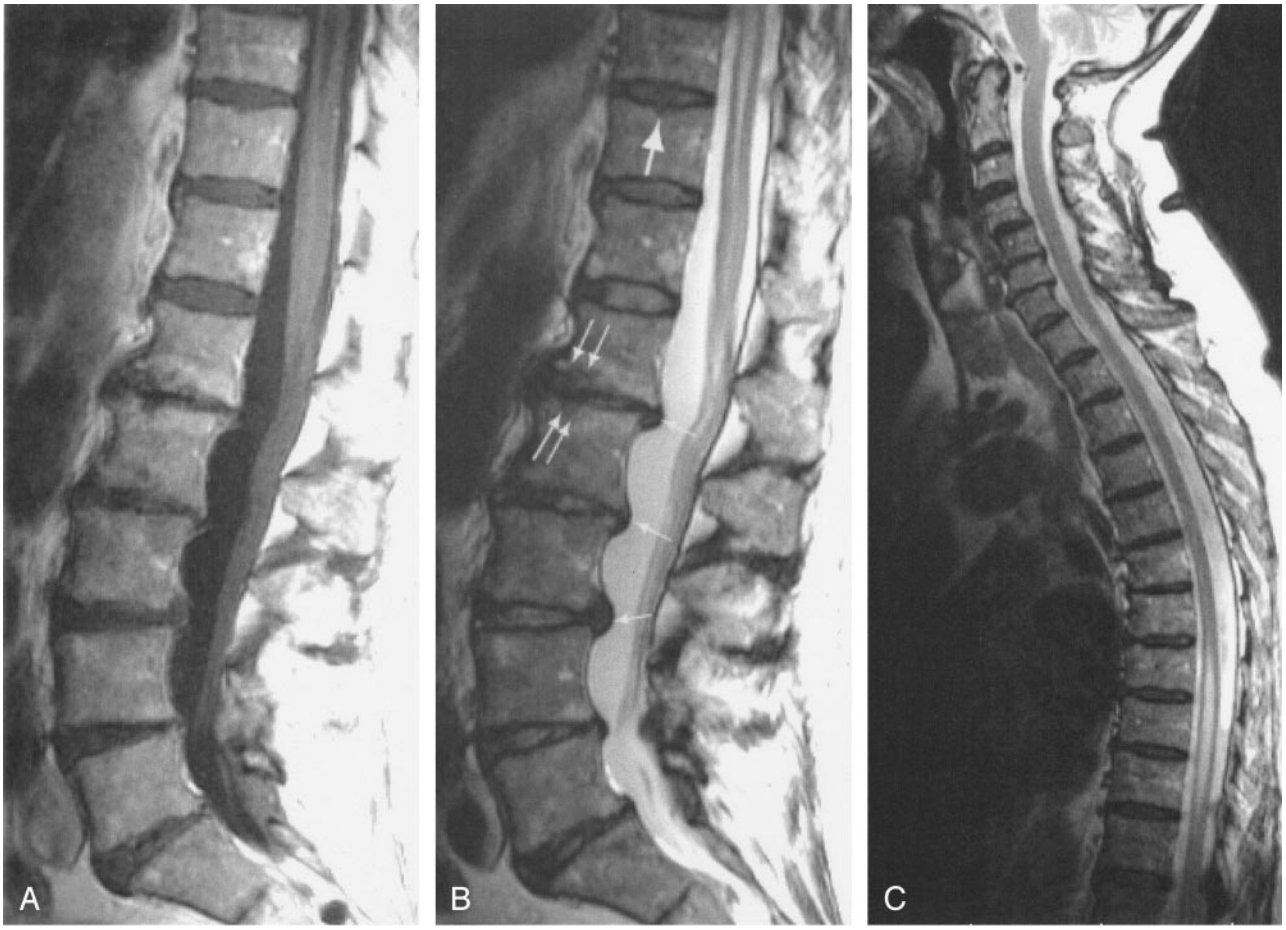

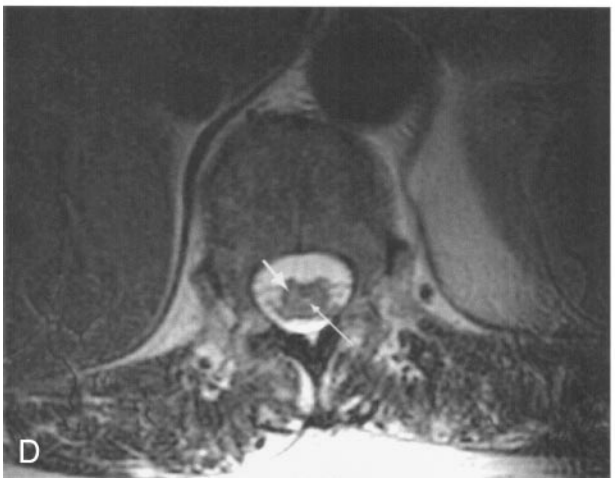

FIG 1. MR imaging examination on admission.

A, Postcontrast midsagittal T1-weighted spin-echo image shows caudal extremity of the HSM cavity and thin linear enhancement of the epithelial lining of the ependymal canal within the conus. Cord parenchyma does not enhance.

B, Midsagittal T2-weighted fast spin-echo (FSE) image of the lumbosacral spine shows thin longitudinal central conal hyperintensity corresponding to enhancing linear area in panel *A* and slightly increased signal intensity of the conus. Disk protrusions (*thin arrows*), chronic osteoarthritic changes (*paired arrows*), and small Schmorl nodes (*thick arrow*) are present.

C, Midsagittal T2-weighted FSE image of the cervicodorsal segment shows upward extension of the incident HSM cavity to Th7-Th8. The cord cephalad to this level is normal.

D, Transverse T2-weighted FSE image at the T12 level shows slightly increased signal intensity of the conal parenchyma, mainly on the right side (*thicker arrow*). Ependymal canal is visible (*thinner arrow*).

cord swelling, enhancement on postcontrast T1-weighted images, and hyperintensity on T2-weighted images are common features to most ischemic, inflammatory, infectious, or tumoral processes (12). In 1991, Mikulis et al (4, 7) described the MR imaging monitoring of a necropsy-proven case of FCE to the spinal cord and highlighted discriminating features: absence of early (day 5) contrast enhancement, but heterogeneous on delayed follow-up examination (day 21); presence of deoxyhemoglobin on day 5 images and of methemoglobin on day 21 images. Pathologic proof of FCE to the cord is rarely available, because most patients presumptively presenting with the condition are surviving and spinal biopsy is rarely considered except for in cases of neoplastic conditions. Some authors have underlined the value of a clinical (radiologic) laboratory entity raising a high probability for the diagnosis by using variable combinations of the following criteria in patients with spinal cord infarction of unknown origin (8–11): minor spinal trauma a few hours or days before the onset of paraplegia; absence of major bone lesion (e.g., fracture, luxation, vertebral body collapse) on radiographic examination (conventional radiograph or CT

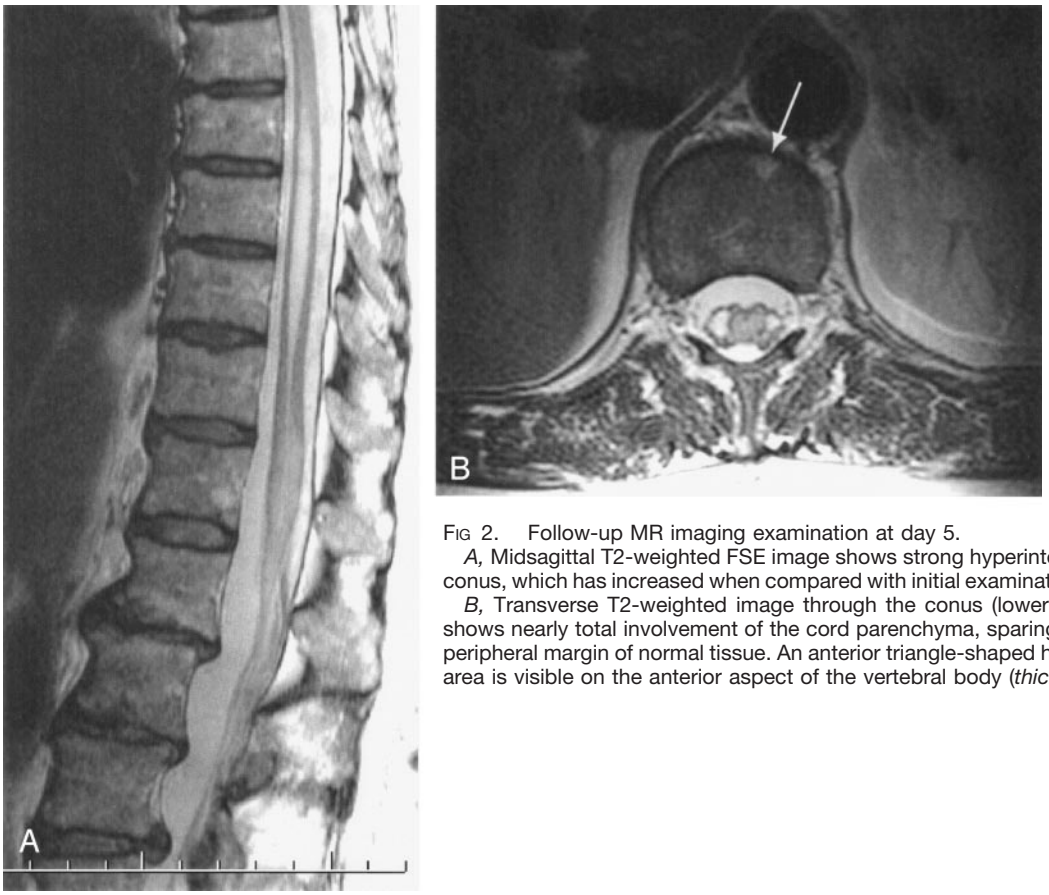

FIG 2. Follow-up MR imaging examination at day 5.

A, Midsagittal T2-weighted FSE image shows strong hyperintensity of the conus, which has increased when compared with initial examination (Fig 1B).

B, Transverse T2-weighted image through the conus (lower Th12 level) shows nearly total involvement of the cord parenchyma, sparing only a thin peripheral margin of normal tissue. An anterior triangle-shaped hyperintense area is visible on the anterior aspect of the vertebral body (*thick arrow*).

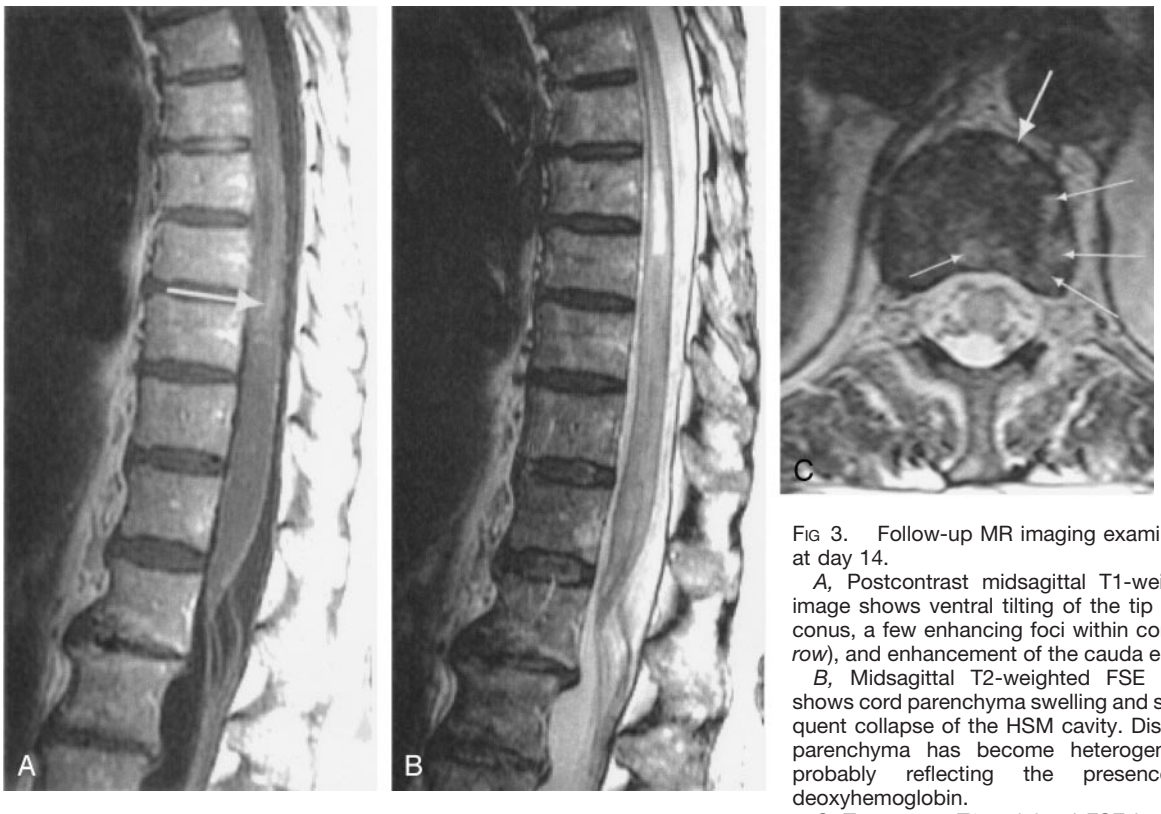

FIG 3. Follow-up MR imaging examination at day 14.

A, Postcontrast midsagittal T1-weighted image shows ventral tilting of the tip of the conus, a few enhancing foci within cord (*arrow*), and enhancement of the cauda equina.

B, Midsagittal T2-weighted FSE image shows cord parenchyma swelling and subsequent collapse of the HSM cavity. Diseased parenchyma has become heterogeneous, probably reflecting the presence of deoxyhemoglobin.

C, Transverse T2-weighted FSE image at the low-T12 level clearly demonstrates the appearance of multiple additional areas of increased signal intensity within the vertebral body (*thin arrows*) when compared with Figure 2B, corresponding to additional foci of acute bone marrow infarction.

FIG 4. Follow-up MR imaging examination at day 25 (72 hours before death).

A, Precontrast midsagittal T1-weighted SE image shows increased signal intensity of the conus, reflecting hemorrhagic necrosis.

B, Postcontrast midsagittal T1-weighted SE image shows enhancement of the pia, but no parenchymal enhancement, probably reflecting increase in endothelial permeability of the pia and decrease in blood supply to the cord.

C, Transverse T2-weighted FSE image through the T11 level shows parenchymal hyperintense foci (*arrows*) representing areas of bland infarction without hemorrhagic transformation

D, Transverse T2-weighted FSE image through the T11-T12 level shows hypointense spots due to the presence of deoxyhemoglobin within the cord (*arrow*) representing areas of hemorrhagic transformation.

scan), but herniation of the nucleus pulposus into the vertebral body through the cartilaginous endplate of the plateaus either in the acute mode or, at least, in the chronic one (Schmorl nodes); intervening symptom-free interval and progressive "stroke-in-evolution" course; and normal CSF examination.

In our case, the patient's daughter reported a benign fall of her mother a few days before. The onset of the complete paraplegia, however, seemed to have occurred suddenly; the time of admission was approximately 6 hours later. The initial MR imaging examination excluded a cord compression but revealed only slight changes within the conus, because the delay between symptoms onset and admission was short (Fig 1). Only usual osteoarthritic changes of the intersomatic and posterior joints were present with chronic disk protrusions and Schmorl nodes, but neither vertebral collapse nor acute intracanalar nucleus pulposus herniation was present (Figs 1 and 2). The causative chronic disk protrusions through cartilaginous endplates may have been located at the L1-L2 level (osteoarthritis) or at the inferior plateau of Th11 (Schmorl node) (Fig 1B). Different mechanisms have been hypothesized to explain the entry of the disk material into the spinal cord microvasculature: 1) lateral rupture of the annulus fibrosus followed by direct penetration of disk material into the adjacent radicular artery; 2) disk material injection into small arteries that are specifically present within degenerating disks or children's disks and retrograde progression to the radicular arteries due to elevated intradiscal pressure; and 3) retrograde migration of degenerated disk material issued from Schmorl nodes into the veins of the vertebral body and thereafter of venous microcirculation of the cord (1, 4). Moreover, spinal arteriovenous communications may result in concomitant arterial and venous embolisms, which are seen in 25% of the cases (4). The rarity of FCE to the spinal cord contrasts with the common finding of osteoarthritic changes and of Schmorl nodes on day-

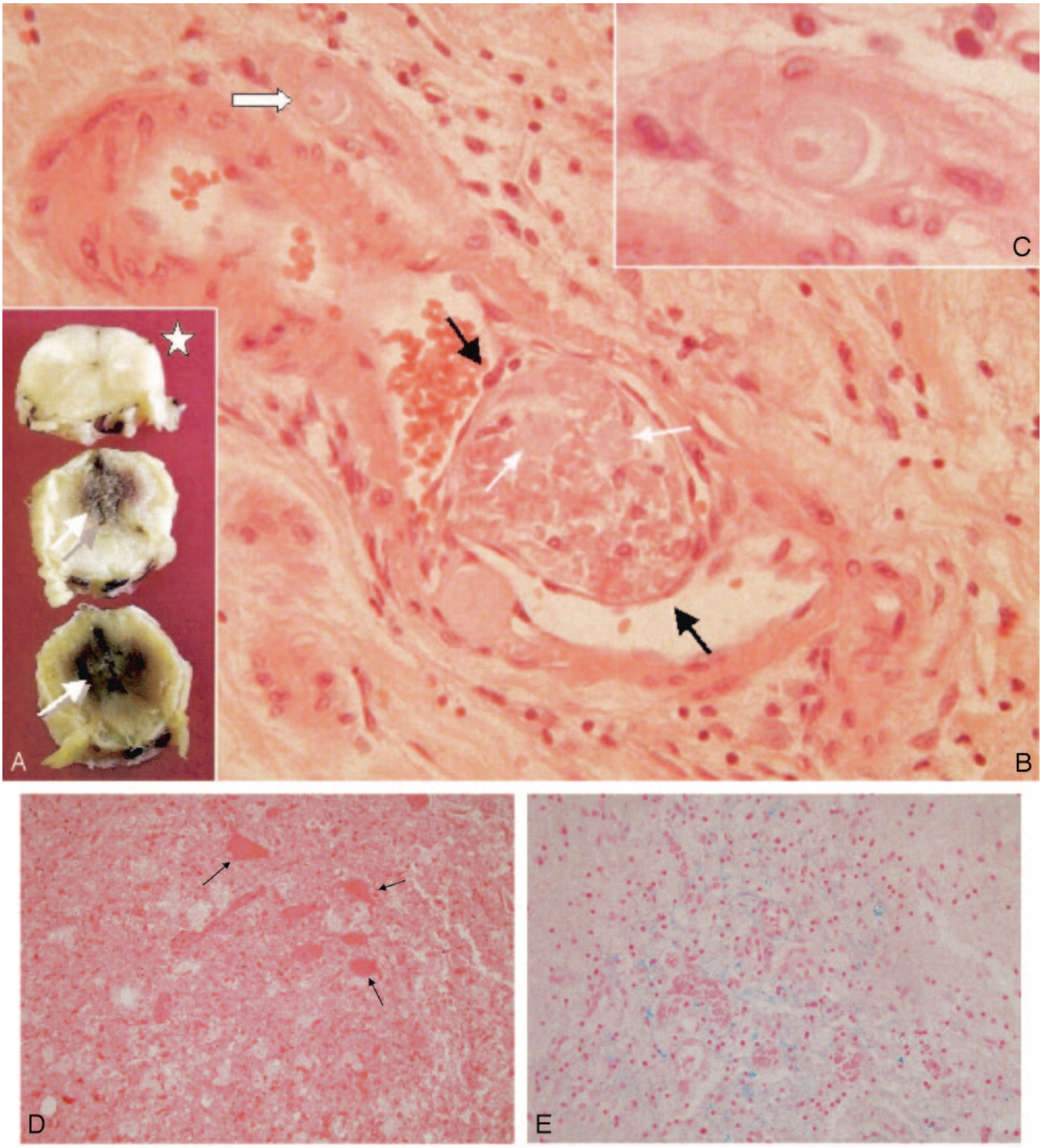

FIG 5. Pathologic examination of necropsic specimen.

A, Macroscopic views of the cord. Necrotic hemorrhagic areas are seen within the lower levels of the thoracic cord (*white arrows*). Upper thoracic level appears unaltered (*star*).

B, Microscopic view. Epithelialized thrombus (*between black arrows*) is observed within a leptomeningeal artery, surrounded by leptomeningeal tissue infiltrated by a few inflammatory cells. Thrombotic material is mostly necrotic, but cartilaginous material can be identified within the clot (*thin white arrows*). A magnified view of a chondrocyte is shown (*C, thick white arrow*).

C, Magnified view of the chondrocyte within a tangentially cut arterial lumen (*B, thick white arrow*).

D, Hematoxylin-eosin staining of anterior horns conal tissue shows necrotic tissue. Dying motoneurones are shown (*arrows*).

E, Perls staining of anterior horns conal tissue shows blue clumps corresponding to hemosiderin deposits and red dots corresponding to "free" red cells.

to-day spinal MR imaging examinations. Colonization of the vertebral body vessels by cartilaginous material thus far appears very uncommon, even in the presence of extensive degenerative or microtraumatic changes. Follow-up examinations revealed concomitant foci of bone marrow infarction within the vertebral bodies, which is a well-documented phenomenon in spinal ischemia (13). In our patient, only small

areas of bone marrow ischemia were observed, which did not result in compromise of the overall mechanical competence of the involved vertebral body (Fig 3C). A blood cord barrier breakdown was observed on follow-up contrast-enhanced images (Fig 3A). A significant switch was observed from homogeneous T2 hyperintensity within diseased cord segments on early images (Fig 2A) to a heterogeneous one on later images strongly suggesting hemorrhagic transformation (Fig 3B). An unusual anterior tilting of the tip of the conus was clearly observed (Fig 3). This may have resulted either from attraction of the conus by periconal and periradicular pia inflammatory changes (*extrinsic* mechanism) or from differences in intensity of edematous changes between anterior and posterior segments of the cord (*intrinsic* mechanism). On the examination 72 hours before death, strongly increased signal intensity was observed within the conus on precontrast T1-weighted images and no parenchymal enhancement was observed on postcontrast images (Fig 4A, B). This suggested hemorrhagic necrosis and interruption of arterial supply of the conal, both of which were confirmed by postmortem pathologic examination (Fig 5). The specificity of these features, even combined, remains low, but it closely matched the only similar case described in the literature by Mikulis et al (4, 7). Absence of contrast enhancement at an early phase, but appearance at a later one, presence of deoxyhemoglobin at an early phase, and of methemoglobin at a later phase are common features to both cases. Complete cord devascularization at the terminal phase, anterior tilting of the conus, cauda equina enhancement, and switch from homogeneous T2 hyperintensity within diseased cord parenchyma to heterogeneous findings were additional features in our case. The definite diagnosis of FCE to the spinal cord still requires histopathologic examination of the diseased cord. Further observations of acute cord syndromes monitored by serial MR imaging may, however, reveal whether the constellation of signs reported here could act as a diagnostic pattern for FCE.

References

1. Naiman JL, Donohue WL, Prichard JS. **Fatal nucleus pulposus embolism of spinal cord after trauma.** *Neurology* 1961;11:83–87
2. Laterre EC. **Syndrome spinal antérieur par embolies multiples de tissu fibrocartilagineux.** *Rev Neurol (Paris)* 1962;106:685–690
3. Tosi L, Rigoli G, Beltramo A. **Fibrocartilaginous embolism of the spinal cord: a clinical and pathogenetic consideration.** *J Neurol Neurosurg Psychiatry* 1996;60:55–60
4. Mikulis DJ, Ogilvy SC, McNee A, et al. **Commentary: spinal cord infarction and fibrocartilaginous emboli.** *AJNR Am J Neuroradiol* 1992;13:155–160
5. Kestle JRW, Resch L, Tator CH, Kucharczyk W. **Intervertebral disc embolization resulting in spinal cord infarction.** *J Neurosurg* 1989;71:938–941
6. Cauzinille L, Kornegay JN. **Fibrocartilaginous embolism of the spinal cord in dogs: review of 36 histologically confirmed cases and retrospective study of 26 suspected cases.** *J Vet Intern Med* 1996;10:241–245
7. Case records of the Massachusetts General Hospital. **Case 5–1991.** *N Engl J Med* 1991;324:322–332
8. Han JJ, Massagli TL, Jaffe KM. **Fibro-cartilaginous embolism: an uncommon cause of spinal cord infarction: a case report and review of the literature.** *Arch Phys Med Rehabil* 2004;85:153–157
9. Raghavan A, Onikul E, Ryan MM, et al. **Anterior spinal cord infarction owing to possible fibrocartilaginous embolism.** *Pediatr Radiol* 2004;28:44–47
10. Davis GA, Klug GL. **Acute-onset nontraumatic paraplegia in childhood: fibrocartilaginous embolism or acute myelitis?** *Childs Nerv Syst* 2000;16:551–554
11. Beer S, Kesselring J. **Fibrocartilaginous embolism of the spinal cord in a 7-year-old girl.** *J Neurol* 2002;249:936–937
12. Cosnard G, Sarrazin JL, Duprez Th. **Méningites, arachnoïdites, myélites et myélopathies.** In: Cosnard G, Lecouvet F, eds. *Imagerie du rachis, des méninges et de la moelle épinière.* 1st ed. Paris: Masson; 2001:129–57
13. Yuh WT, Marsh EE 3rd, Wang AK, et al. **MR imaging of spinal cord and vertebral body infarction.** *AJNR Am J Neuroradiol* 1992; 13:145–154